Effect of storage time, plasticizer formulation and extrusion parameters on the performance of thermoplastic starch films

M. Paula Guarás*, Vera A. Alvarez, Leandro N. Ludueña

Consejo Nacional de Investigaciones Científicas y Técnicas (CONICET), Instituto de Investigaciones en Ciencia y Tecnología de Materiales (INTEMA), Grupo de Materiales Compuestos Termoplásticos (CoMP), Facultad de Ingeniería, Universidad Nacional de Mar del Plata, Av. Colón 10850 (B7606BVZ) Mar del Plata, Argentina

*Corresponding author: Tel: (+54) 223 626 0600; E-mail: paula.guaras@gmail.com, luduenaunmdp@gmail.com, alvarezvera@gmail.com

Abstract

A twin screw extrusion processing method was developed for the preparation of thermoplastic starch (TPS) for packaging applications. Different plasticizer combinations were used looking for the minimal temperature profile in the extruder in order to prevent the thermal degradation of TPS. The effect of storage time at 25 °C and 50% of relative humidity on the properties of TPS was studied. Plasticized TPS samples observed by scanning electron microscopy showed homogeneous fracture surfaces without unstructured starch granules. X-ray diffractometry tests showed retro gradation of all TPS formulations with progressive Vh-type crystal structure formation. Temperature for maximum thermal degradation rate of raw materials was shifted to higher values after preparing the TPS, suggesting not only physical but also chemical interactions between plasticizers and starch molecules. Mechanical properties were significantly improved replacing 10 wt. % of glycerol by water as plasticizer, which was attributed to the increased gelatinization degree and the reduction of thermal degradation. Copyright © 2019 VBRI Press.

Keywords: Thermoplastic starch, processing condition, formulation, storage time.

Introduction

Petrochemical based polymers such as polyethylene (PE), polypropylene (PP), polystyrene (PS), among others; have been increasingly used as packaging materials, owing to relatively low cost and mechanical and vapor/oxygen barrier properties that fulfill the requirements of this application. These materials are fully recyclable but for some applications such as thin films in contact with food, recycling is not easy to be performed. This situation and the non-biodegradable characteristic of these materials, has caused a major environmental problem regarding the disposal of waste [1].

Currently there is a growing interest in the use of biodegradable polymers with similar functionalities and process abilities than traditional petrochemical-based polymers. Biodegradable polymers refer to polymeric materials that are capable to undergoing decomposition into carbon dioxide, methane, water, inorganic compounds, or biomass in which the predominant mechanism is the enzymatic action of microorganisms, that can be measured by standardized tests, in a specific period of time [2]. Among natural and biodegradable polymers, thermoplastic starch has been considered as one of the most promising candidates because of an attractive combination of availability, price, process ability and performance [3].

Native starch (NS) is the term used for the starch extracted from agro-resources such as maize, wheat, rice, cassava, potatoes, among others. NS has a granular morphology with different sizes and shapes, and is composed of amylose and amylopectin in different quantities depending on its source [4]. NS is partially crystalline with granules of 120-140 nm thick altering amorphous and semi-crystalline rings arrangement [5]. Its granules show birefringence when they are subjected to polarized light, which demonstrate its molecular organization [6]. The main advantage of native starch as a material includes its abundance, low cost, renewability and biodegradability [7]. Compared to synthetic polymers, NS has two main disadvantages: A) NS contains hydroxyl groups which impart hydrophilic properties. The amylose is dissolved in water and amylopectin swells in presence of water. So the starch disintegrates in water and loses its properties when exposed to moisture [8]. B) The structure of native starch must be modified, since its thermal degradation starts at a temperature below than its melting point. For this reason native starch cannot be processed by conventional plastics technology without any modification. This modification is performed by the breakdown of the starch granule when it is processed in the presence of a specific amount of plasticizer, at a given extrusion conditions [9]. This process is called

gelatinization and the obtained product is known as thermoplastic starch (TPS).

TPS is not at equilibrium, in fact exhibits time-dependent-changes in its macroscopic properties and structure, associated with storage conditions. This process is known as retrogradation which is related with a recrystallization phenomenon [10]. There are several factors that affect this process such as moisture and temperature of environment, plasticizer formulation, ratio of amylose and amylopectin, among others. Storage time always affects the crystallinity of the material and its glass transition temperature, which produce changes in mechanical and barrier properties [11-14]. TPS properties can be stabilized after a certain period of time at controlled storage conditions, but after that period they will significantly change if the material is submitted to different humidity conditions mainly due to the high susceptibility of its properties to absorbed moisture [15]. Both, time-dependence and moisture susceptibility of TPS on its final properties should be minimized for packaging applications.

Schmitt *et al.* [16] have studied the effect of storage time and plasticizers on the structural stability of melt processed TPS synthesized from wheat starch. They found that mechanical properties during ageing are highly dependent on the plasticizer composition. Thus, through different plasticizer combinations and ageing, starch-based materials with significant differences in tensile properties can be obtained. Jiménez *et al.* [36] studied the addition of fatty acids (FA) into starch films containing glycerol as plasticizer, in order to reduce the hygroscopic character of the films and to improve water vapour permeability. They found that he degree of starch and FA crystallinity increased with storage time and gave rise to changes in film properties: films became stiffer, less effective as water vapour barriers and less transparent and glossy, evidencing that the retro gradation process took place in the sample. Esmaeili *et al.* [32] in his work study the influence of the combination of two different plasticizers in the mechanical, thermal, chemical properties and resistant to retro gradation. They obtained an increase in the properties using a mixture of glycerol and sorbitol as a plasticizer and high resistance to retro gradation. Battegazzore *et al.* [10] prepared TPS from maize starch using isosorbide as an innovative bio-based and biodegradable plasticizer. They probed by X-ray diffractometry and dynamic-mechanical thermal experiments the absence of retro gradation after 9 months of storage at 50% relative humidity. On the other hand, they did not study the effect of storage time on the mechanical and thermal properties. López *et al.* [17] compared the effect of conventional plasticizers (glycerol/water) and non-conventional ones (alginate/glycerol) on the thermal and mechanical properties of TPS from maize starch prepared by melt mixing. Non-tacky films were obtained using alginate/glycerol as plasticizer, while those obtained with water/glycerol showed a sticky appearance. They found that alginate allows maintaining the plasticizing effect avoiding, at the same time, the main disadvantages associated to the use of water during starch melting process. Typical properties for packaging applications such as mechanical and barrier ones were not studied in that work. Lara *et al.* [18] studied the impact of different glycerol/water proportions on the gelatinization and retrogradation processes of TPS from cassava starch. The gelatinization process was carefully controlled in a rotational rheometer with solvent trap. Oscillatory rheological tests at a fixed frequency of 1.0 Hz and a fixed strain of 5% were performed applying a temperature ramp from 20 °C to 160 °C at a heating rate of 5 °C/min. They monitored the evolution of elastic (G´) and viscous (G´´) moduli during the process to determine the gelatinization temperature. They used this information to analyze the effect of nanoclays on the different gelatinization mechanisms. They showed that clays significantly increase the gelatinization temperature depending on the plasticizer formulation.

From these works, it can be concluded that the processing strategy (equipment and processing parameters) and plasticizer composition should be studied simultaneously in order to optimize the quality of the TPS products. In addition, a twin screw extrusion process at pilot plant scale should be designed taking into account the high flow rate involved in any industrial processing line for plastic packaging products. Then, the study of the effect of storage time on mechanical properties is required as a tool for selecting the optimal TPS formulation for packaging applications.

The aim of this work is to design a twin screw extrusion process at pilot plant scale to prepare TPS films with optimized mechanical properties and water vapor absorption for packaging applications. The physical/chemical structure, mechanical/thermal properties and water absorption of TPS during storage at 25 °C and 50% of relative humidity (RH) for a period between 0-9 months will be analyzed.

Experimental

Materials

Maize starch as powder form with oval to polyhedral granules in shape and apparent amylose content of ~19% [19] (named NS) provided by "Distribuidora Dos Hermanos, Mar del Plata, Argentina". The plasticizers used were glycerol (99% purity, purchased from "Química DEM, Mar del Plata, Argentina") and distilled water. Stearic acid supplied by SA Shuchardt Merck OHG was used as a lubricant for processing.

Preparation of thermoplastic starch

Gelatinization of starch was performed in an intermeshing co-rotating twin-screw extruder "Doble Argentina" with a twin bore barrel each bore with diameter (Db) of 25 mm and a barrel length (Lb) to Db

ratio of 25. **Fig. 1** shows a scheme of the twin screw extruder.

The extruder has 5 independent heating control systems. Thermocouples are located in the positions denoted as T1, T2, T3, T4 and T5 in **Fig. 1**. The die consists of 3 capillaries with a diameter (Dd) of 3 mm and a length (Ld) of 20 mm. Vacuum/venting port was only used as venting. Side feeding system was not used.

Raw materials (69.5 wt% of native starch, 0.5 wt.% of stearic acid and 30 wt.% of plasticizer) were premixed in a beaker and then feed into the main extruder hopper. **Table 1** shows the formulation of the plasticizer and the different temperature profiles used from the feed zone to the die. The speed of the co-rotating screws was set at 50rpm obtaining flow rates between 1 to 2 kg/h. The strands (~3mm diameter) going out from the die were air cooled at 20 °C and guided downstream up to the pelletizer located 5m far away from the extruder die. Then, rectangular films of 150x200 mm^2 with thickness of 1.14±0.03 mm were obtained by compression molding following the next procedure: 10 min at 120 ºC and 0 kg/cm^2, 10 min at 120 ºC and 50 kg/cm^2, and finally mold cooling with water up to 30 °C. Materials were storage at 50% RH from the time the films were prepared, and were tested at different stages during aging (1 week, 1 month, 4 months and 9 months).

Characterizations

Optical microscopy (OM)

Native starch granules were observed in an optical microscopy Leica DM LB. A solution of 0.1 g of NS in 10ml of distilled water was casted onto a microscopy slide. Finally a second slide was placed above the sample and polarized light was used to observe the granules morphology.

Scanning electron microscopy (SEM)

SEM micrographs of the crio-fractured surface of the TPS samples were taken with a JEOL JSM-6460 LV instrument. The samples were prepared by cutting 10mm×20mm rectangular specimens after the immersion in liquid air to avoid the plastic deformation of the observed surface. Samples were observed after 1 week of the extrusion process.

X-ray diffractometry (XRD)

The X-Ray patterns were obtained in an Analytical Expert Instrument equipment (K∞Cu=1.54 Å) from 2θ = 2º to 60º (2 º/minute) at 20 °C. The generator voltage was 40 kV and the current was 40 mA.

Thermogravimetric analysis (TGA)

Thermogravimetric tests were carried out with a Shimadzu TGA-50. Samples were heated at a constant rate of 10 °C/min from room temperature to 700 °C, under nitrogen atmosphere. The temperatures for maximum degradation rates of TPS components were calculated from the derivative thermogravimetrical analysis (DTGA).
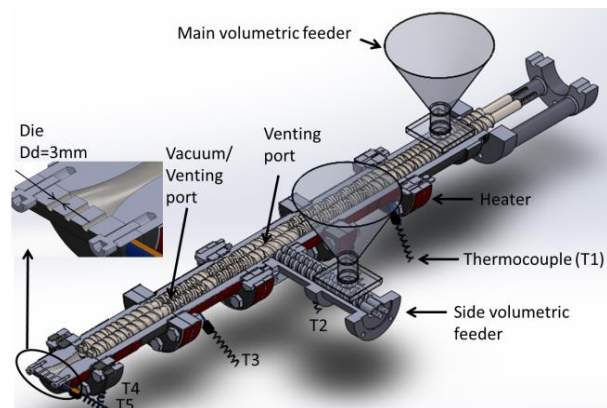

Fig. 1. Scheme of the twin screw extruder.

Table 1. Formulations of plasticizer and temperature profiles in the extruder.

Material	Plasticizer (wt.%)	Temperature profile (T1/T2/T3/T4/T5) (°C)	Film sample
TPS1	100 Glycerol	90/100/110/120/120	
TPS2	100 Glycerol	80/90/100/110/100	
TPS3	90Glycerol+ 10water	80/90/100/110/100	
TPS4	90Glycerol+ 10water	70/85/100/110/100	

Differential scanning calorimetry (DSC)

Differential scanning calorimetry tests were carried out in a Perkin Elmer Pyris 1DSC. About 8 mg of the samples were accurately weighed into aluminum pans and sealed hermetically. The samples were cooled down to −80 °C, and then heated to 250 °C at a heating rate of 10 °C/min under nitrogen atmosphere. Finally, they were cooled down to room temperature.

Water vapor absorption (WVA)

Water vapor absorption experiments were performed on square specimens of 20 mm^2. Prior to the water absorption measurements, the samples were dried in a vacuum oven at 30-35 ºC for 48 h. The samples were conditioned in hermetic containers at 20 °C with 90% relative humidity, using a solution of glycerin and water. The amount of water absorbed by the samples was calculated by weighing them periodically, until a constant weight was attained. The water uptake (W) was given by the following equation:

$$W(\%) = \frac{M_t - M_0}{M_0} * 100$$

$$(1)$$

where, M_t is the weight at time t and M_0 is the initial weight. Equilibrium water absorption (W_{eq}) was calculated from the maximum absorbed water of the plots W as a function of $t^{1/2}$.

Water vapor permeability (WVP)

Water vapor permeability (WVP) was calculated following the guidelines of the ASTM E96 standard, using the Dry Method. Samples were placed in cylindrical acrylic cells 39 mm in diameter, which contained calcium chloride previously dried in an oven at 150 °C for 24 hours. Disc-shaped samples were used to seal the dry chamber. Cells were placed in a chamber at room temperature (22 °C) and controlled relative humidity (65.4%RH), and their weight was periodically recorded.

The calculation of WVP was made by the following method:
- Water vapor transmission was calculated by the following equation:

$$WVT = \left(\left(\frac{G}{t}\right) * e\right)/A \qquad (2)$$

where, G is the variation of weight at a given time (g), t is the time at which G (h) occurs, (G / t) slope of weight as a function of time (g / h), e is the thickness of the sample, A is the permeation area of the sample (m^2) and WVT is the water vapor transmission (g / h.m^2).
- Water vapor permeability (WVP) was calculated by the flollowing ecuation:

$$WVP = \frac{WVT}{S.(R_1 - R_2)} \qquad (3)$$

where, S is the saturated vapor pressure at test temperature (mmHg), R_1 is the relative humidity fraction of the source (for the dry method corresponds to the humidity of the chamber), R_2 is the relative humidity fraction in the steam sump (calcium chloride), WVP is the water vapor permeability (g / Pa.s.m^2).

Measurements were taken after an initial equilibrium period to ensure steady-state diffusion. At least six measurements of each sample were made.

Mechanical testing

The tensile tests were performed according to the ASTM D882 on an INSTRON 4467 machine using a load cell of 100 N and operating at a constant crosshead speed of 1 mm/min. Prior to mechanical measurements, the samples were conditioned at 60% relative humidity for 48 h at 20 °C.

Results and discussion

Morphological analysis (SEM, XRD): Gelatinization, microstructure stability and retrogradation

The simplest technique to analyze the gelatinization degree after extrusion is the scanning electron microscopy. **Fig. 2** shows the SEM images of native starch by OM and TPS by SEM.
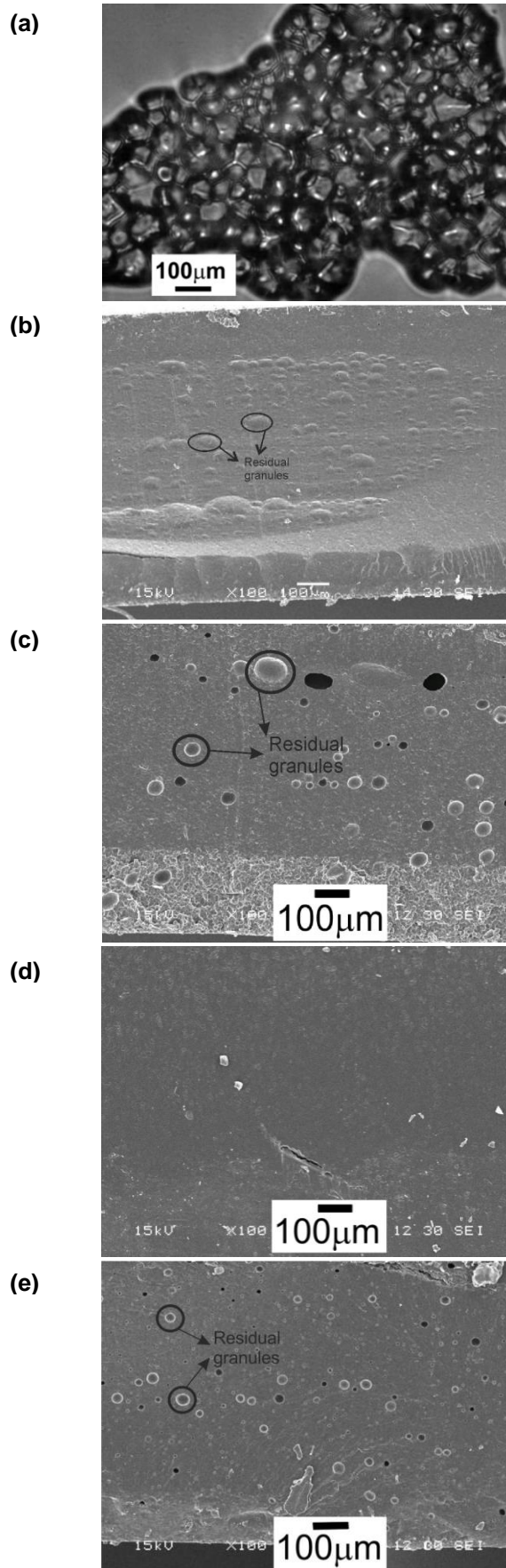

Fig. 2. OM of native starch and SEM micrographs of the cryo-fractured surface of all TPS samples after 1 week from extrusion: (a) Native Starch, (b) TPS1, (c) TPS2, (d) TPS3, (e) TPS4.

It is known that a continuous phase observed in the cryo-fractured surface is an indication of complete gelatinization while residual native starch granules dispersed in the continuous phase indicates an incomplete de-structuration of starch granules [**1**]. It is possible to observe that starch granules are still present in TPS1, TPS2 and TPS4. TPS3 is the only material for which complete gelatinization was achieved. Comparing TPS1 and TPS2, both with 30wt. % of glycerol as plasticizer, TPS2 showed more residual starch granules which is attributed to the decreased temperature profile in the extruder. Similar tendency was obtained comparing TPS3 and TPS4. They had the same plasticizer composition but higher extruder temperature profile in the case of TPS3, for which residual starch granules were not observed by SEM. Although higher extruder temperature profile was used in TPS1 in comparison with TPS3, residual starch granules were observed in TPS1. This result can be attributed to the partial replacement of glycerol by water as plasticizer. It should be noted the relevance of this result since complete NS gelatinization at lower temperatures in an extrusion process is always preferred for thermal degradation in the final product.

Another technique used to analyze the effectiveness of the gelatinization process is the X-ray diffractometry. The data collected from this characterization can be also used to study the microstructure stability and retrogradation [**10, 16, 18**]. Depending on their source, native starches have different X-ray diffraction patterns known as A, B and C forms. Native starches with A and B-type crystalline microstructure have double helical, six-fold structures. The packing density of the double helices in the unit cell is the main difference between these forms. Native starches from cereals usually have A-type diffractograms, while starches from roots and amylose-rich presents B-type diagrams. The C-type structure is thought to be an intermediate situation between A and B-type and are typical for legume native starches [**20, 21**].

When native starch granules are destructured after the gelatinization process by heat and shear forces, i.e. processing by double screw extrusion, amylose, which is an essentially linear polymer, leaves the granules and it was shown that can crystallize in different crystalline structures known as V_a, V_h and E_h-type. In the case of cereal native starches these structures arise from complexes formed between amylose and lipids [**22**]. On the other hand, amylopectin, which is a branched polymer, crystallizes into the B-type form during retrogradation [**23**].

Table 2 shows the 2θ positions reviewed from literature corresponding to the XRD characteristic peaks of the different crystalline forms (A, B, C, V_a, V_h, E_h-types) that may appear in native and thermoplastic starch X-ray diffractograms [**24-31**].

Fig. 3 shows the X-ray plots for the native starch and for TPS1 as a function of storage time at 50%RH. Similar plots were obtained for TPS2, TPS3 and TPS4.

Table 2. 2θ position for the different possible crystalline structures present in native and thermoplastic starch.

Type	A	B	C	V_a	V_h	E_h
	14.8s*	5.5m	14.8s	7.9s	7.5s	6.9m
	16.6vs*	10.8m	16.8v	13.4vs	13.0vs	12.0m
	17.7s	14.8s	17.6m	13.6vs	13.3s	18.4s
	22.6vs	17.0vs	22.6s	15.8m	14.9w	
2θ (°)	26.3w*	19.3s	30.2w	19.4m	17.0m	
	30.1m*	22.1vs	33.5w	20.8vs	18.8m	
	33.2w	23.8s		26.3w	19.8vs	
		26.1w			22.2m	
		30.9w			22.6m	
		34.0m			25.2m	

* Qualitative intensity: vs = very strong; s = strong; m = medium; w = weak.
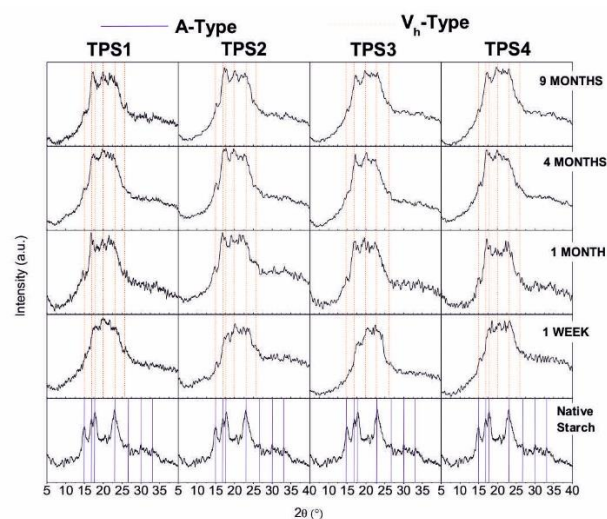

Fig. 3. X-ray diffraction diagrams of native maize starch and the different TPS formulations as a function of storage time.

In the case of native starch an A-type crystalline structure can be recognized. Same result was obtained by Esmaeili *et al.* [**32**] for maize starch. It was reported that the A-type crystal structure of maize starch is transformed to V_a-type crystal structure just after plasticization using glycerol and/or water as plasticizer. V_a-type crystals are unstable and can be transformed to V_h-type during storage, also known as retrogradation [**32**]. Changes in the intensity of all or some peaks corresponding to the same crystalline structure can also be attributed to retrogradation [**33**]. It can be seen in **Fig. 3** that the strong peak of native starch around 14.8° is transformed into a weak peak while the very strong peak of native starch at 16.6° is transformed to a medium intensity peak at similar positions (± 0.4°) for all TPS samples at 1 week. This transformation can be attributed to V_h-type crystal structure formed after gelatinization [**10**]. It is also possible to see that the intensity of these peaks increased from 1 week to 1 month of storage and then remained almost constant

after 4 and 9 months. The increased intensity at these 2θ positions for TPS can be attributed to progressive V$_h$-type crystal structure formation during retrogradation which seems to be stopped at some time between 1 week and 1 month of storage [**1**]. The strong peak for native starch at 17.7°, which is strictly related to A-type structure, is absent for TPS3 but still present for TPS1, TPS2 and TPS4 which can be attributed to incomplete gelatinization also shown by SEM. A very strong peak at 19.8° is present in the plots of all TPS formulations and its intensity did not significantly change as a function of storage time. This peak was not observed in native starch patterns and is attributed to V$_h$-type structure. Native starch also shows a very strong peak at 22.6° corresponding to A-type crystals. This peak is transformed to a medium intensity one for all TPS formulations but its intensity does not change as a function of time indicating transformation to V$_h$-type. Finally, a peak at 25.2° was observed for all TPS plots with increasing intensity as a function of time but it was not present in native starch one. This peak is attributed to V$_h$-type structure and it gives evidence of retrogradation in the TPS samples.

Some concluding remarks from morphology analysis can be established. First, it was proved by SEM and XRD that TPS3 was the only combination of plasticizer type/content and processing conditions that was able to produce complete gelatinization. This phenomenon was attributed to the partial replacement of glycerol by water. This strategy was mainly designed to decrease the temperature profile along the extruder in order to prevent TPS thermal degradation. Regarding XRD analysis, retrogradation was confirmed from changes in the intensity of the peaks corresponding to TPS V$_h$-type crystalline structure. Retrogradation seems to stop at some time between 1 week and 1 month of storage since variations in the position and intensity of the peaks were not observed from 1 to 9 months of storage for any TPS formulation. Retrogradation of TPS from V$_a$-type to V$_h$-type crystalline structure was not observed so it was assumed to take place during the first week of storage. In future works XRD characterization at few hours after the gelatinization will be performed in order to verify retrogradation from V$_a$-type to Vh-type structure. Because of the hydration of the samples, after nine month the formation of B-type crystallinity is promoted. The confirmation of retrogradation makes necessary the study of mechanical/thermal properties and water absorption as a function of time since final properties of TPS strongly depend on its crystalline structure [**3-10**].

Thermal properties

The DTGA plots of the raw materials and the different TPS samples are shown in **Fig. 4**.

The DTGA plots of TPS show three steps of thermal degradation. The first one represents the evaporation/dehydration that starts when the temperature rises at 90 ºC. The second step corresponds to the degradation of glycerol and stearic acid, with a temperature of maximum rate of thermal degradation (T$_d$) at ~280 °C, which is overlapped with the beginning of the third step that corresponds to starch degradation. T$_d$ for glycerol in TPS shifted to higher temperatures (~284 °C) than those for the neat glycerol (~264 °C). This result suggests not only physical but also chemical interactions between glycerol and starch. Similar result was obtained by Shi *et al.* for citric acid/glycerol co-plasticized thermoplastic maize starch [**34**]. The thermal stability of native starch (Td=314 °C) did not significantly change after gelatinization since Td remained around 316±4 °C for all TPS samples and storage times analyzed. On the other hand, the thermal degradation process of all components in TPS did not show significant variations as a function of processing temperature, plasticizer formulation nor storage time.
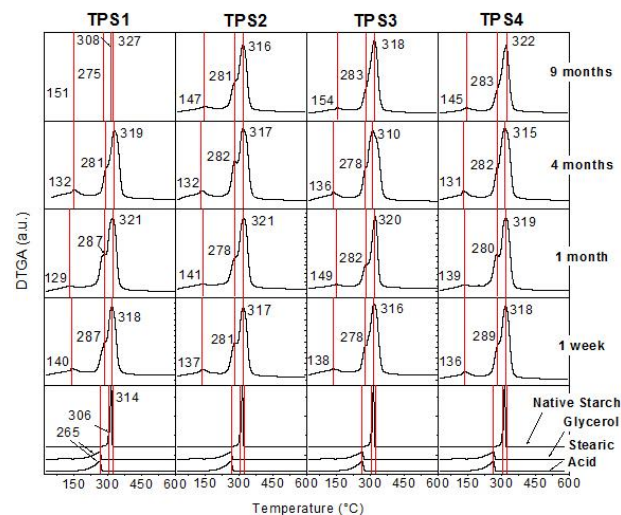

Fig. 4. DTGA plots of raw materials and TPS samples as a function of storage time (numbers inside the plots correspond to the temperatures [°C] of the main peaks).

Fig. 5a shows the DSC graph for TPS4 after 1 week of storage indicating the methodology for calculation of glass transition temperature (Tg). Similar curves were obtained for all formulations and storage times. **Fig. 5b** shows the Tg values for all TPS samples as a function of storage time.
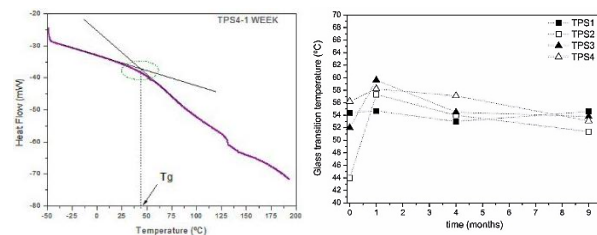

Fig. 5. (a) DSC curve showing the methodology for calculating the Tg of the material. (b) Glass transition temperature of the TPS samples as a function of storage time calculated from DSC.

Chung *et al.* [**35**] concluded that when the starch-based samples are stored below their Tg and have enough time to reach thermodynamic equilibrium, Tg values begin to decline. This result is consistent with the retrogradation results obtained by XRD between

1 week and 1 month of storage. It was shown that retrogradation stops after 1 month of storage at a temperature below the Tg. This result suggests that 1 month is the time needed to reach a stable crystalline structure. During the first month of storage; small V_h-type crystalline regions may be continuously forming also acting as physical crosslinking points which limit the movement of molecules. So, higher temperatures will be required for the chain segment to move which causes Tg to increase. The slight reduction of Tg observed from 1 to 4 months of storage is attributed to the increased water uptake as will be shown in the next section. Water is an efficient plasticizer for TPS causing reduction on Tg. Tendencies from 4 to 9 months of storage are not clear and may be the result of a balance between gelatinization and crystallinity degrees, crystalline morphology and water uptake.

Observing the Tg values for the different materials, at constant storage time, it can be concluded that tendencies change depending on the analyzed time. Several parameters such as degree of gelatinization, crystallinity, type of crystalline structure, plasticizer formulation and water uptake may be acting simultaneously and changing in different proportions as a function of storage time leading to the observed results.

Finally, it is interesting to remark that Tg is in the range of 56 °C ± 4 °C for all materials and storage times which may be a problem for packaging applications when packed products are stored at high room temperatures. Properties may significant change as the room temperature approach to Tg values.

Water absorption

TPS has a great tendency to absorb or desorb water being this issue the major drawback in the use of this kind of materials for packaging products because of the significant dependence of mechanical properties on it [**15**]. Water absorption tests were carried out at 90% RH. At first, it was observed that all the samples for each storage times reached absorption equilibrium after two weeks. **Fig. 6** shows the equilibrium water absorption (W_{eq}) of all materials as a function of storage time.
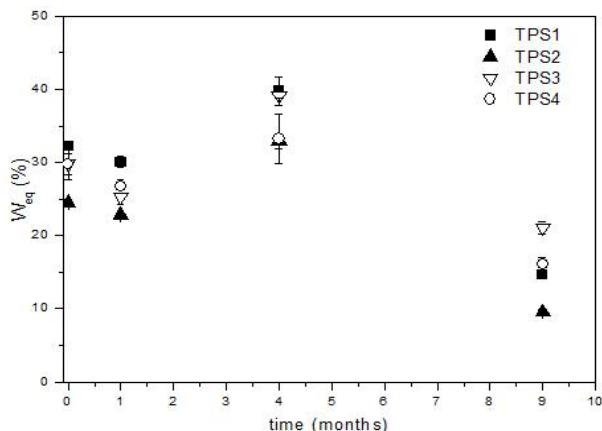

Fig. 6. Equilibrium water absorption as a function of storage time for all TPS formulations.

It can be observed that the tendencies on W_{eq} between the different materials depend on the storage time analyzed, as was observed for Tg in the previous section. Same parameters having effect on Tg (degree of gelatinization, crystallinity, type of crystalline structure, plasticizer formulation) may be also changing water vapor absorption behavior. On the other hand, it can be seen that after 4 months of storage the W_{eq} increased which probably caused the reduction of Tg, observed in Tg experiments, at the same storage time.

Mechanical properties

Stress-strain curves of TPS3 at different stages of aging are shown in **Fig. 7**.
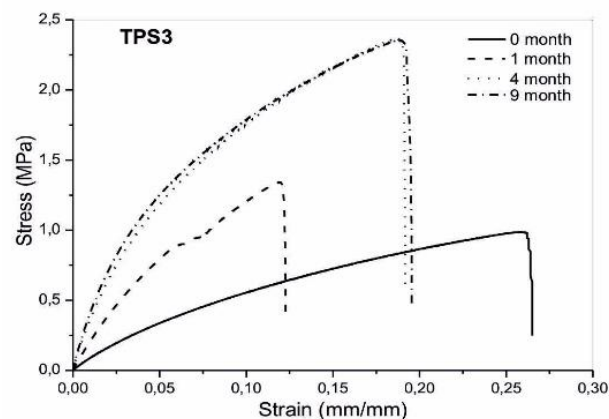

Fig. 7. Stress-strain curves of TPS3 obtained at different storage times.

The shape of the curves was similar for all materials and storage times analyzed showing a typical pattern of rubbery materials [**36**].

Fig. 8 shows the Young´s modulus, maximum tensile stress and elongation at break of all TPS as a function of storage time.

It can be observed that the materials that were extruded with low temperature profile (TPS2 and TPS4) showed lower Young´s modulus, maximum tensile stress and elongation at break. This result can be mainly attributed to the incomplete gelatinization process.

Replacing 10 wt.% of glycerol by water in the formulation of the plasticizer increased all mechanical properties. It can be attributed to the improved gelatinization and minimization of thermal degradation of starch during the process. The magnitudes of these improvements were different depending on the storage time analyzed. Mechanical properties of TPS depends on several parameters such as degree of gelatinization, crystallinity, type of crystalline structure, retrogradation, starch source, chemical structure, glass transition temperature and equilibrium water absorption. It was probed in the previous sections that most of these parameters depend not only on the plasticizer type and extrusion parameters but also on the storage time, mainly due to retrogradation. Final

mechanical properties will be the result of a balance between these TPS characteristics for each storage time analyzed. TPS3 was the material with best combination of Young´s modulus, maximum tensile stress and elongation at break for all storage times. It showed 250%, 114% and 34% of increment on Young´s modulus, maximum tensile stress and elongation at break, respectively, after 9 months of storage.
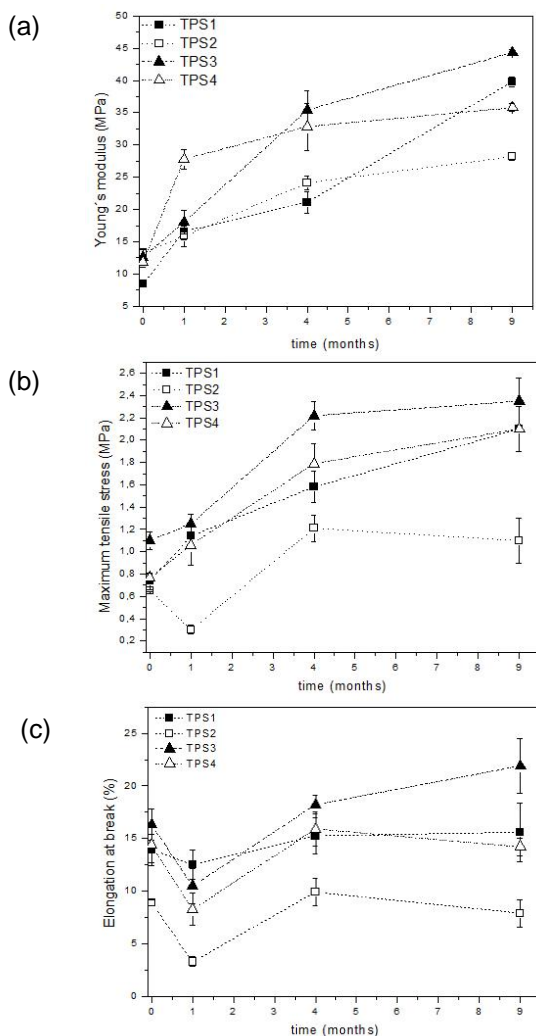

Fig. 8 Mechanical properties of all TPS formulations as a function of storage time: (a) Young´s modulus, (b) maximum tensile stress (c) elongation at break.

Conclusion

A twin screw processing line was successfully developed for the preparation of TPS derived from maize starch at pilot plant scale. The replacement of 10 wt. % of glycerol by water in the formulation of the plasticizer was an efficient strategy to obtain a completely gelatinized TPS structure. It also allowed decreasing the temperature profile in the extruder barrel minimizing thermal degradation of TPS during the gelatinization process. X-ray diffractometry showed the presence of retrogradation for all TPS formulations with progressive formation of V_h-type crystalline

structure between 1 week and 1 month of storage at 20 °C and 50% RH. Increased Tg and decreased equilibrium water absorption observed between 1 week to 1 month of storage was attributed to retrogradation. Tendencies on these properties between 4 and 9 months of storage were not clear and attributed to a balance between gelatinization and crystallinity degrees and crystalline morphology. Thermal stability of raw materials was improved after preparing TPS suggesting not only physical but also chemical interactions between plasticizers and TPS molecules. Mechanical properties (Young´s modulus, maximum tensile stress and elongation at break) were significantly improved at all storage times by replacing glycerol by water in the plasticizer formulation and minimizing the temperature profile in the extruder barrel to the limit of complete gelatinization.

The selected material was the TPS prepared with 30 wt% of plasticizer (90 wt.% glycerol and 10 wt.% distiller water) and an extruder barrel temperature profile of 80/90/100/110/100 °C. This material showed improvements on mechanical properties which is important considering the final application. It showed improvements from 14 to 317% on these properties in comparison with those of TPS will worst mechanical performance. It should also be taken into account that retrogradation is found in all formulations. This fact limits the effective time of use of the material. However, the values of Tg limit the use of the material in places where the ambient temperature is higher than 40 ℃, since the material could present structural changes. The optimized TPS formulation will be used in future works looking for further improvements on mechanical and barrier properties and to improve the stability of these properties over the storage period at different relative humidifies looking for the replacement of commodities for packaging applications. The strategies to be work with will contemplate chemical modification of native starch by esterification with maleic anhydride and the incorporation of nanoclays to the TPS matrices.

References

1. Firwan, M.J., Strawbridge; *Food Packag. Technol.*, **2003**, 174.
   DOI:10.1002/9781444392180.ch7
2. ASTM, D6400-99; **2002**, U.S. PA 19428-12959.
3. Shogren, R.L.; *Carbohydr. Polym.*; **1992**, *19,* 83.
   DOI: 10.1016/0144-8617(92)90117-9
4. Souza, R.; Andrade, C.T.; *J. App. Polym. Sci.*; **2001**, *81,* 412.
   DOI: 10.1002/app.1453
5. Hoover, R.; *Carbohydr. Polym.*; **2001**, *45,* 253.
   DOI: 10.1016/S0144-8617(00)00260-5
6. Thire, R.; Simao, R.A.; Andrade, C.T.; *Carbohydr. Polym.*; **2003**, *54,* 149.
   DOI: 10.1016/S0144-8617(03)00167-X
7. Wilhem, H.M.; *Carbohydr. Polym.*, **2003**, *54,*149.
   DOI:10.1016/S0144-8617(02)00239-4
8. Carvalho, A.; Curvelo, A.; Agnelli, J.; *Carbohydr. Polym.*; **2001**, *45,*189.

9. Cajiao, S., *Univ. EAN Facultad de Posgrados espec. gerencia de proyectos Bogotá*; **2012**.
10. Battegazzore, D.; *Carcohydr. Polym.*, **2015**, *119,*78.
    DOI:10.1016/j.carbpol.2014.11.030
11. Smits, A.L.; *Starch/Stärke*, **1998**, *50,* 478.
    DOI: 0038-9056/98/1212-0478$17.50+.50/0
12. Lu, T.; Jane, J.; Keeling, P.L.; *Carbohydr. Polym.*, **1997**, *33,* 19.
    DOI: 10.1016/S0144-8617(97)00038-6
13. Soest, J.J.; Vliegenthart, J.F.; *Trends Biotechnol.*, **1997**, *15,* 208.
    DOI: 10.1016/S0167-7799(97)01021-4
14. Shi, R.; *J. App. Polym. Sci.,* **2007**, *103,* 574.
    DOI: 10.1002/app.25193
15. Nafchi, A.M.; *Starch/Stärke*, **2013**, *65,* 61.
    DOI:10.1002/star.201200201
16. Schmitt, H.; *Carcohydr. Polym.*, **2015**, *115,* 364.
    DOI: 10.1016/j.carbpol.2014.09.004
17. Lopez, O.V.; *Carcohydr. Polym.*, **2015**, *126,*83.
    DOI:10.1016/j.carbpol.2015.03.030
18. Lara, S.C.; Salcedo, F.; *Carbohydr. Polym.*, **2016**, *151,* 206.
    DOI: 10.1016/j.carbpol.2016.05.065
19. Gutierrez, T; Alvarez, V.A.; *React. Funct.Polym. k,* **2017**, *112,* 33.
    DOI: 10.1016/j.reactfunctpolym.2017.01.002
20. Katz, J.R.; Itallie, V.; *Physik. Chem.*, **1930**, *150,* 90.
21. Zobel, H.F., *Starch/Stärke*, **1988**, 40, 44.
    DOI: 0038-9056/88/0202-0044$02.50/0
22. Bail, P.L., *Biopolymers*, **1999**, *50,* 33.
    DOI: 10.1002/(SICI)1097-0282(199907)50:1<99::AID BIP9>3.0.CO;2-A
23. Lourdin, D.; *Polymer*, **1997**, *38,* 5401.
    DOI:0032-3861/97/$17.00 + 0.00
24. Rappenecker, G; Zugenmaier, P.; *Carbohydr. Res.*, **1981**, *89,* 11.
    DOI: 0008-621518110000-0000/S 02 50
25. Zobel, H.F.; French, A.D.; Hinckle, M.E.; *Biopolymers*, **1967**, *5,* 837.
    DOI: 10.1002/bip.1967.360050906
26. Brisson, J.; Chanzy, H.; Winter, W.T., *Int. J. Biol. Macromol.*, **1991**, *13,* 31.
    DOI: 0141-8130/91/010031~9
27. Winter, W.T.; Sarko, A.; *Biopolymers*, **1974a**, *13,* 1461.
    DOI:10.1002/bip.1974.360130716
28. Winter, W.T.; Sarko, A.; *Biopolymers*, **1974b**, *13,* 1447.
    DOI: 10.1002/bip.1974.360130715
29. Mercier, C., *Cereal Chem.*; **1980**, *57,*4.
30. Yamashita, Y; Monobe, K.; *J. Polym. Sci. Part A2*, **1971**, *9,* 1471.
    DOI:10.1002/pol.1971.160090807
31. Buleon, A; *Int. J. Biol. Macromol.,* **1990**, *12,* 25.
    DOI: 2410620
32. Esmaeili, M; Pircheraghi, G.; Bagheri, R.; *Polym. Int.*, **2017**, *66,* 809.
    DOI:10.1002/pi.5319
33. Shanks, R.A.; Wasantha, L.M.; Gunaratne, K.; *J Therm Anal Calorim*; **2011**, *106,* 93.
    DOI:10.1007/s10973-011-1620-8
34. Shi, R.; *Carbohydr. Polym.*, **2007**, *69,* 748.
    DOI:10.1016/j.carbpol.2007.02.010
35. Chung, H. J.; Seung-TaikLim; *Food Hydrocolloids*; **2003**, *17,* 855.
    DOI:10.1016/S0144-8617(03)00077-8
36. Soest, J., *Carbohydr. Polym.*, **1996**, *29,* 225.
    DOI:10.1016/0144-8617(96)00011-2
37. Jiménez A.; *Food Hyd.*, **2012**, *26,* 302.
    DOI:10.1016/j.foodhyd.2011.06.009